



# HHS Public Access

Author manuscript

*Calcif Tissue Int.* Author manuscript; available in PMC 2018 January 18.

Published in final edited form as:

*Calcif Tissue Int.* 2015 January ; 96(1): 65–72. doi:10.1007/s00223-014-9928-6.

## Primary Cilia Exist in a Small Fraction of Cells in Trabecular Bone and Marrow

**Thomas R. Coughlin,**

Tissue Mechanics Laboratory, Bioengineering Graduate Program, University of Notre Dame, Notre Dame, IN, USA

**Muriel Voisin,**

Department of Mechanical and Biomedical Engineering, National University of Ireland, Galway, Galway, Ireland

**Mitchell B. Schaffler,**

Department of Biomedical Engineering, Grove School of Engineering, City College of New York, New York, USA

**Glen L. Niebur,** and

Tissue Mechanics Laboratory, Bioengineering Graduate Program, University of Notre Dame, Notre Dame, IN, USA

**Laoise M. McNamara**

Department of Mechanical and Biomedical Engineering, National University of Ireland, Galway, Galway, Ireland

### Abstract

Primary cilia are potent mechanical and chemical sensory organelles in cells of bone lineage in tissue culture. Cell culture experiments suggest that primary cilia sense fluid flow and this stimulus is translated through biochemical signaling into an osteogenic response in bone cells. Moreover, in vivo, primary cilia knockout in bone cells attenuates bone formation in response to loading. However, understanding the role of the primary cilium in bone mechanotransduction requires knowledge of its incidence and location in vivo. We used immunohistochemistry to quantify the number of cells with primary cilia within the trabecular bone tissue and the enclosed marrow of ovine cervical vertebrae. Primary cilia were identified in osteocytes, bone lining cells, and in cells within the marrow, but were present in only a small fraction of cells. Approximately 4 % of osteocytes and 4.6 % of bone lining cells expressed primary cilia. Within the marrow space, only approximately 1 % of cells presented primary cilia. The low incidence of primary cilia may indicate that cilia either function as mechanosensors in a selected number of cells, function in

---

Correspondence to: Laoise M. McNamara.

Thomas R. Coughlin and Muriel Voisin have contributed equally to this work.

**Conflict of Interest** Thomas R. Coughlin, Muriel Voisin, Mitchell B. Schaffler, Glen L. Niebur, and Laoise M. McNamara have no conflicts of interest to disclose.

**Human and Animal Rights and Informed Consent** This article does not contain any studies with human or animal subjects performed by any of the authors.

concert with other mechanosensing mechanisms, or that the role of primary cilia in mechanosensing is secondary to its role in chemosensing or cellular attachment.

## Keywords

Mechanobiology; Mechanotransduction; Primary cilia; Marrow; Osteocyte; MSCs

---

## Introduction

Bone adapts to mechanical loading through the coordinated activities of osteocytes, osteoblasts, and osteoclasts. Osteoblasts and osteocytes are derived from marrow stromal cells (MSCs), while osteoclasts are derived from hematopoietic stem cells (HSCs) [1]. MSCs, HSCs, and their progeny reside in the trabecular bone marrow forming a complex multicellular niche [2, 3], while osteocytes are entombed within the mineralized bone. All of these cells are subjected to mechanical cues due to skeletal loading [4].

MSCs, osteoblasts, osteocytes, and osteoclasts are all mechanosensitive and both intra- and intercellular signaling are driven by a range of mechanical loads [5]. However, the precise mechanisms of mechanosensation are unknown. Osteocytes are exposed to fluid flow in vivo [6], and respond to fluid flow in culture by producing biochemicals and proteins associated with osteogenic differentiation [7–9]. MSCs and osteoblasts also respond to fluid flow, intercellular forces, and matrix strain in vitro [10, 11], and may be subjected to these stimuli in vivo [12]. A number of mechanosensing cellular structures that could sense these signals have been proposed [13], including ion channels, gap junctions [14], integrins [15], and the actin cytoskeleton [16]. Recently, primary cilia have been cited as a potential important mechanosensor in bone cells and MSCs [16, 17].

Primary cilia are cell appendage organelles formed during the quiescent/G1 phase of the cell cycle, and are comprised of nine microtubule doublets that attach to the basal body and are encased in the plasma membrane [18–21]. Primary cilia sense and respond to mechanical cues in many cell types, most notably acting as essential flow sensors in the epithelial cells of the kidney [22]. When the cilium bends in response to flow, an influx of  $\text{Ca}^{2+}$  occurs and spreads to neighboring cells [23].

Recent studies have implicated primary cilia in bone cell mechanotransduction. In vitro, primary cilia inhibition in MSCs blocks osteogenic gene transcription, but increases MSC proliferation [17]. Primary cilia abrogation [16] or inhibition [24] in MC3T3-E1 osteoblasts also attenuates normal osteogenic responses to fluid flow. Primary cilia abrogation in MLOY4s abolishes upregulation of osteogenic factors normally experienced in response to fluid flow in vitro [16, 24]. In vivo, mice with an osteoblast- and osteocyte-specific knockout of Kif3a, a gene essential to primary cilia formation and function, exhibited bone formation in response to loading, but it was diminished compared to control mice [25]. Conditional knockout of Kif3a also decreases the number and length of primary cilia in osteoblasts, which results in osteopenia [26]. In addition to its role as a mechanosensor, primary cilia are known to facilitate various physiological functions including chemical sensory processes [27] and matrix attachment [28]. Moreover, the length of cilia decreases in response to

mechanical loading in both tenocytes [29] and chondrocytes [30], suggesting that cilia may respond to local matrix deformation, as the fluid flow velocities are small in these models.

The role of primary cilia as mechanosensors in bone cells *in vivo* depends on the types and numbers of cells with cilia, and their local mechanical environment. In particular, primary cilia in osteocytes may sense fluid flow through the lacunar-canalicular network [6]. However, there are conflicting reports regarding *in vivo* expression of cilia in osteocytes in cortical bone. Tonna and Lampen found primary cilia in only 4 % of osteocytes in aging mice using transmission electron microscopy (TEM) [31], while 94 % of osteocytes in rat tibia exhibited immunohistochemical staining for the primary cilia marker, acetylated  $\alpha$ -tubulin [32]. In the trabecular bone compartment, the incidence of ciliated osteocytes in bone tissue and ciliated cells in the bone marrow space is not known. In bone marrow, cells with elongated cilia may be preferentially located in areas of the marrow where they are likely to be subjected to mechanical or chemical stimuli. For example, near the trabecular bone marrow interface, cells are subjected to high shear stresses during physiological loading [4], and biochemical signals between osteocytes, bone lining cells, and osteoblastic precursors in the marrow are prevalent. As such, quantifying the presence of primary cilia in the trabecular bone and marrow may lend understanding to their role as mechano- or chemosensors or indicate other putative functions. While osteocytes are believed to reside in a mechanically stimulated environment [6], where mechanotransduction via cilia is possible, cells in the centralized marrow may not experience as much mechanical stimulation. Intercellular motion in the marrow cavity is primarily driven by bone deformation, which would deform and displace cells attached to the bone and their immediate neighbors. As such, presentation of an elongated cilia in the central bone marrow, where such motion would be attenuated, may not be beneficial. The goal of this study was to determine the fraction of cells expressing primary cilia in trabecular bone osteocytes, in marrow cells near the bone surface, and in cells in the central marrow cavity. In order to achieve this, we validated an immunostaining protocol for sheep trabecular bone and marrow; and applied it to quantify the number and length of cilia within the marrow, on the bone surface, and within the bone matrix.

## Materials and Methods

### Animal Model

Primary cilia expression was studied in trabecular bone from the cervical vertebrae of young sheep, 6 to 8 months of age. The sheep is a grazing animal and bone from this site would be subjected to regular cyclic loading from the neck musculature. Ovine kidney was studied as a positive control for the antibodies. Bone and kidney were obtained from an abattoir (Brady's, Athenry, Ireland) within four hours of the time of slaughter, and maintained on ice throughout processing.

### Antibody Validation

To verify the specificity of the antibodies in ovine tissue, we conducted preliminary staining on kidney and bone. Acetylated  $\alpha$ -tubulin and intraflagellar transport protein 88 (IFT88), both of which are vital for ciliogenesis [21], were used to target primary cilia.

Antibody specificity was verified in the kidney, a tissue where primary cilia are known to be present [33]. The tissue was fixed in 4 % w/v paraformaldehyde (PFA) for 72 h and cut into small sections that were processed (Leica ASP300) and paraffin embedded (Leica EG1150H). Longitudinal sections were cut at 20  $\mu\text{m}$  using a microtome (Leica RM2235), collected on SuperFrost® slides (Menzel Glaser), and left to dry overnight at 60 °C. Slides were stored at room temperature, until dual immunostaining as described below. Slides were imaged using a Nikon confocal microscope.

Paraffin-embedded samples were rehydrated as per routine protocols (xylene and descending grades of ethanol) and were stained after proteinase K antigen retrieval (20  $\mu\text{g}/\text{mL}$  in TE buffer, 20 min at 37 °C). Slides were rinsed twice for 2 min with 0.5 % v/v Phosphate Buffered Saline (PBS)-Tween and blocked for 1 h with 3 % Normal Goat Serum (NGS)/1 % Bovine Serum Albumin (BSA) in PBS.

For acetylated  $\alpha$ -tubulin staining, blocked sections were incubated with anti acetylated  $\alpha$ -tubulin (Abcam), 1/20 dilution in NGS 3 %/BSA 1 % in PBS, overnight in a humidified chamber at 4 °C, followed by three 10 min rinses in BSA 1 % w/v in PBS. Goat Dylight 488 anti mouse 1/200 (Jackson ImmunoResearch) secondary antibody was then applied for 1 h at room temperature in a dark humidified chamber. Three 10 min rinses with BSA 1 % w/v in PBS were performed in the dark and slides were mounted with a fluoroshield mounting media (Sigma) containing propidium iodide (PI) as a nuclear counterstain with coverslips (#1 thickness, Menzel Glaser). For dual immunostaining, anti acetylated  $\alpha$ -tubulin, at 1/20 dilution, was targeted with goat anti mouse Dylight 594 (Jackson ImmunoResearch), at 1/200 dilution, and then anti IFT88 (Santa Cruz), at 1/100 dilution, as a second primary antibody targeted with Dylight 488, at 1/200 dilution. Dual immunostained slides were counterstained with 4',6-diamidino-2-phenylindole (DAPI) nuclear stain with cover-slips. The antibody specificity validation was repeated in trabecular bone. One of the three ovine trabecular bones harvested from the cervical vertebrae was selected for dual immunostaining. The samples were harvested, processed, and immunostained using acetylated  $\alpha$ -tubulin and IFT88, as described in detail above.

### **Cilia in Isolated Marrow Stromal Cells**

Marrow cells were extracted from the trabecular bone marrow of three ovine cervical vertebrae using centrifugation and expanded to passage three on collagen coated (Sigma) slides. On four consecutive days of expansion, subpopulations of MSCs were fixed using 4 % w/v PFA for 20 min, permeabilized for 5 min at 4 °C (2 mM sodium chloride (NaCl), 1.5 mM magnesium chloride ( $\text{MgCl}_2$ ), 16 mM sucrose, and 0.5 % Triton X in PBS), and immunostained with anti acetylated  $\alpha$ -tubulin similar to the method described above using anti acetylated  $\alpha$ -tubulin at 1/50 dilution.

### **Cilia in Trabecular Bone and Marrow**

Three cylindrical cores of trabecular bone and marrow were obtained from the C2 vertebrae of three sheep. The end plates of the vertebrae were removed, and cylindrical cores were prepared using an 8.25 mm hollow diamond-tipped drill bit (Starlite) under constant irrigation. The cores were fixed in 4 % w/v PFA for 48 h and demineralized for 21 days

using 10 % w/v ethylenediaminetetraacetic acid (EDTA) buffered to a pH of 7.5 at 4 °C. After demineralization, samples were rinsed in dripping tap water overnight to drain excess EDTA. Processed and paraffin-embedded samples were sectioned at 20 µm, collected on SuperFrost® slides, and left to dry overnight at 60 °C. Slides were stored at room temperature. The sections were immunostained for acetylated  $\alpha$ -tubulin as described above.

### Confocal Microscopy

Slides were imaged on an inverted confocal laser-scanning microscope (LSM 510; Zeiss, Germany). Because the slides had multiple labels, multitracking was used to reduce bleaching and bleed through. The image acquisition software used was AIM 4.2 (Zeiss, Germany). Low-magnification (10 $\times$ ) and high-magnification (63 $\times$ , oil immersion objectives) micrographs were obtained using a low scan speed (7 s), averaging 4 images, using a 1024  $\times$  1024 pixel definition. An argon laser (488 nm) was used to excite Dylight 488, and a Neon laser (550 nm) was used to excite PI.

For dual immunostained slides, a fluorescent Revolution confocal microscope (Andor), with spinning disk (Yokagawa CSU22) was used. The software used was Andor iq 2.3 acquisition software (Andor). Low- and high-magnification (10 $\times$  and 63 $\times$  oil immersion objectives, respectively) micrographs were obtained using a low scan speed, averaging 4 images, using a 1004  $\times$  1002 pixel definition. An argon laser (488 nm) was used to excite Dylight 488, a Neon laser (561 nm) was used to excite Dylight 561, and an ultraviolet light (350 nm) was used to excite DAPI.

False color imaging was used to generate micrographs. Image stacks were acquired at 63 $\times$  magnification, using a 0.5-µm step, and an average of four images per optical slice were taken. This step was chosen, as it was small enough to capture cilia of the most commonly reported length, but was large enough to limit the acquisition time to not bleach the section. For imaging the marrow, two randomly selected marrow pores were imaged per section, generating three to five image stacks per pore. When imaging the bone matrix, five randomly selected areas were acquired per section.

### Primary Cilia Assessment

Primary cilia were quantified under confocal microscopy in three locations in each bone: in the marrow space away from the endosteal surface (marrow >50 µm from the bone wall), marrow near the endosteal surface (marrow <50 µm from the bone wall), and in osteocytes (Fig. 1a–d). Cells near the bone surface were further divided to identify primary cilia in bone lining cells. Image stacks were analyzed using ImageJ software (NIH). Primary cilia were identified based on the presence of stained acetylated  $\alpha$ -tubulin proximal to a nucleus. Cilia measurement depended on their orientation. Cilia oriented in plane with each slice were measured using ImageJ (NIH) and cilia oriented perpendicular to each slice were measured by counting the number of slices they appeared on. The length of primary cilia was measured in three dimensions by combining the measured lengths in three orthogonal directions by the Pythagorean theorem. Because we were interested in cilia that were extended, only stained cilia at least 1 µm in length were counted. Positive acetylated  $\alpha$ -

tubulin was excluded if there were two adjacent stained structures pointing toward one another, indicating two cells at a late stage of mitosis.

To determine the percentage of cells with primary cilia, the number of cells in the different locations was quantified. The number of cells in a marrow region was found using Automatic Nuclei Counter on ImageJ software (NIH). The number of bone lining cells on the trabecular bone surface and osteocytes in trabecular bone were counted directly.

## Results

### Antibody Validation

In ovine kidney tissue, anti IFT88 was colocalized with anti acetylated  $\alpha$ -tubulin on cilia-like structures (Fig. 2a), and the stains were not observed separately. In the absence of either primary antibody, only small regions of diffuse staining by the secondary antibodies were observed (Fig. 2c). Similarly, IFT88 and anti-acetylated  $\alpha$ -tubulin were colocalized and specific in sections of trabecular bone (Fig. 2b). As such, the anti acetylated  $\alpha$ -tubulin antibody was specific to cilia in ovine tissue.

In cultured MSCs, 25 % of 299 cells observed exhibited positive staining for acetylated  $\alpha$ -tubulin (Fig. 2d, e). Cilia were observed on the apical side of cells, extending into the media.

### Primary Cilia Occurrence in Marrow and Trabecular Bone

Primary cilia greater than 1  $\mu\text{m}$  in length were observed in all locations that were analyzed within the trabecular bone samples (Fig. 3a–c). In the marrow, cilia protruded into the intercellular space (Fig. 3a, b). In the bone matrix, cilia appeared in the lacunae adjacent to osteocyte nuclei (Fig. 3c). A total of 13,752 marrow cells at a distance further than 50  $\mu\text{m}$  from the bone wall, 4,983 marrow cells within 50  $\mu\text{m}$  of the bone wall, 758 cells on the bone surface, and 642 osteocytes were analyzed. The percentage of cells with primary cilia (mean  $\pm$  SD) in the marrow space away from the endosteal surface was  $0.91 \pm 0.20$  %. Near the endosteal surface, the percentage was  $1.48 \pm 0.74$  %, and increased to  $4.60 \pm 1.80$  % when only considering bone lining cells. Similarly,  $4.04 \pm 1.04$  % of osteocytes presented primary cilia. A greater percentage of osteocytes and bone lining cells presented primary cilia than did marrow cells in the interior of the pores ( $p < 0.05$ ; Fig. 4).

On average, the measured cilia were 1.62- $\mu\text{m}$ -long, with cilia within the marrow reaching up to 7  $\mu\text{m}$ . The mean length of cilia only differed between osteocytes and marrow cells near the bone surface, while the lengths did not differ between the other locations (Fig. 5).

## Discussion

In this study, we found that cells with primary cilia were rare in trabecular bone and the encompassed marrow space. As such, if cilia are important mechanosensory or chemosensory organelles, then those cells expressing them must be uniquely located to sense and act on these signals. The greater proportion of bone lining cells and osteocytes that expressed cilia compared to cells in the central marrow cavity is consistent with this idea, as osteocytes and marrow cells near the bone are known to affect bone

mechanobiological adaptation and reside in mechanically stimulated areas [4, 6, 12]. The relatively small number of primary cilia in osteocytes and bone marrow cells may indicate that they do not function as mechanosensors in osteocytes or MSCs or that only a small number of MSCs and osteocytes are responsible for sensing loading-induced fluid flow using cilia. Taken together, the primary cilium may be only one of several mechanosensory structures with only a subset of cells relying on them at a given time.

This study provides the first measure of primary cilia incidence in trabecular bone and bone marrow, and also in the bone of large animals. Since cilia may play different roles in cortical versus trabecular bone, in normal versus elevated loading conditions, or across species, it is essential to quantify their presence to fully understand their function. The methods employed to detect and measure cilia in this study were carefully validated, and should be applicable across a range of species and anatomic sites. Indeed, the validation of the antibodies in the ovine model provides further evidence of the conservation of cilia-specific proteins across species.

Some minor limitations of this study must be considered. Foremost, the phenotype of ciliated cells in the marrow and bone tissue was not characterized. While osteocytes embedded in bone tissue can be identified based on their morphology and physical location, the marrow contains cells of both the hematopoietic and mesenchymal lineage. Although we did not identify specific cell types that expressed cilia in the marrow, we did analyze the marrow near the trabecular bone surface separately. This region likely contains osteoprogenitor cells [34], committed osteoblasts, osteal macrophages [35], and HSCs, which are believed to reside adjacent to the bone lining cells [36]. In addition, it is known that proliferation and recruitment of osteoprogenitors occurs close to the trabecular bone surface in the marrow [37]. Although these are only general guides to the cell phenotypes in each region, the large number of cells analyzed made the use of rigorous identification, as with in situ hybridization, unfeasible. There are limitations to immunohistochemistry when staining thick tissue sections. In this case, thick sections of twenty microns were used in order to obtain complete cells in the bone marrow and whole osteocytes in the bone. However, we found that in a randomized subset of marrow image stacks,  $60 \pm 24\%$  of the cilia counted were in the top upper half of the section, while  $40 \pm 24\%$  were in the bottom lower half of the section ( $p = 0.04$ ). Even with this decreased penetration, the percentage of the cells with cilia is accurate, as the fraction of cells in the marrow with cilia would only increase by approximately 0.25% to just more than 1% if we assumed the same antibody penetration into the bottom half as the top half of the sections. In osteocytes, there was no penetration bias, as 50% of the osteocytes were stained in the upper top half and lower bottom half of our sections. This may have perhaps been due to the multicellular nature of the marrow compared to the sparsely populated nature of osteocytes in bone.

The relatively low incidence of cilia in bone marrow stromal cells harvested from these bone samples is comparable to recent reports. From 30 to 60% of cells were reported to have cilia in human adipose-derived stem cells [27]. In contrast, MSCs, MC3T3-E1s and MLO-Y4s demonstrated a high incidence of primary cilia in cell culture [16, 38] in other studies. These latter reports may be reflective of murine cells, or differences in media used to culture the various cell lines [27].

Previous *in vivo* measurements of primary cilia expression in osteocytes have produced conflicting results. Primary cilia were detected in only 4 % of osteocytes in aging mice using TEM [31], which is similar to the results presented here. In contrast, 94 % of osteocytes in rat cortical bone expressed primary cilia based on acetylated  $\alpha$ -tubulin immunostaining [32]. However, subsequent TEM analysis conducted as part of that same study [32] revealed that mother and daughter centrioles without any cilia-like appendages were present in most of the osteocytes. Only 3 of 29 cells examined by TEM exhibited a cilia-like structure interacting with the cell membrane, and few exhibited even an incomplete axoneme [1]. We only measured cilia that were at least 1  $\mu\text{m}$ , which, according to the TEM analysis, is longer than the basal structures associated with the axoneme. It is also important to note that previous studies quantified primary cilia in osteocytes of cortical bone in rodents, while the focus of our study was trabecular bone of the ovine model and its marrow. Trabecular and cortical bone respond differently to mechanical loading [39] and also have different mechanical properties [40]. These differences may be explained by the disparity in cilia presence in trabecular and cortical bone osteocytes that we report. Finally, in cultured ovine cells, fewer cilia are expressed than in other species [41]. As such, differences in both site and species should be considered carefully when applying these results.

The length of cilia measured in this study is comparable to previous reports for cultured cells. Cilia ranged from 1 to 4  $\mu\text{m}$  in cultured chondrocytes [42], 4–9  $\mu\text{m}$  in MC3T3-E1 [16], and 2–4  $\mu\text{m}$  in MLO-Y4 cells [43]. We found that the cilium length varied slightly across locations in the trabecular bone compartment that we analyzed. Although cilium length was up to 7  $\mu\text{m}$  in the marrow near the bone surface and less than 3.5  $\mu\text{m}$  in the rest of the marrow, the average cilium length did not differ between the locations in the marrow. Short cilia in osteocytes may be explained by the spatial constraints of the pericellular space [44]. Similarly, in the marrow, short cilia may be due to spatial restrictions in the intercellular space. Cells can alter the length of their primary cilia [45], which may also explain the small number of cilia greater than 1  $\mu\text{m}$  in length. For example, in fresh tendon, the average length of cilia in tenocytes was 1.1  $\mu\text{m}$ , but increased to 3.0  $\mu\text{m}$  after 24 h in media [29]. Interestingly, subsequent dynamic loading resulted in reduced cilia length similar to fresh tendon [29]. Thus, the short cilia observed in our study may reflect that the cells reside in a mechanically stimulated environment. Similarly, primary cilia increase their length in response to low intracellular calcium levels and vice versa, indicating that calcium levels may be high in the trabecular bone compartment [45].

Overall, this study reveals that primary cilia occur in a small fraction of cells in the trabecular bone and marrow. Our *in vivo* data provide a link between *in vitro* data on primary cilia expression and how they are expressed in the native *in vivo* cellular environment. The low incidence of primary cilia may indicate that (1) cilia function as mechanosensors on a selected number of cells or (2) cilia function in concert with other mechanosensing mechanisms. This study is the first to examine primary cilia incidence in the bone marrow microenvironment. Studying mechanosensors in their multicellular niche to explore mechanosensing is crucial in developing an understanding of mechanotransduction.



## Acknowledgments

This research was supported by grants from Science Foundation Ireland 07/EN/E015B Travel Fellowship T.R.C., European Research Council (ERC) Grant No. 258992 (BONE-MECHBIO) L.McN. and M.V., NSF CMMI-110207 T.R.C. and G.L.N.

## References

1. Owen M. The origin of bone cells in the postnatal organism. *Arthritis Rheum.* 1980; 23:1073–1080.
2. Gurkan UA, Akkus O. The mechanical environment of bone marrow: a review. *Ann Biomed Eng.* 2008; 36:1978–1991. [PubMed: 18855142]
3. Weiss L. The hematopoietic microenvironment of the bone marrow: an ultrastructural study of the stroma in rats. *Anat Rec.* 1976; 186:161–184. [PubMed: 984472]
4. Birmingham E, Grogan JA, Niebur GL, McNamara LM, McHugh PE. Computational modelling of the mechanics of trabecular bone and marrow using fluid structure interaction techniques. *Ann Biomed Eng.* 2013; 41:814–826. [PubMed: 23519534]
5. Birmingham E, Niebur GL, McHugh PE, Shaw G, Barry FP, McNamara LM. Osteogenic differentiation of mesenchymal stem cells is regulated by osteocyte and osteoblast cells in a simplified bone niche. *Eur Cell Mater.* 2012; 23:13–27. [PubMed: 22241610]
6. Knothe Tate ML. “Whither flows the fluid in bone?” An osteocyte’s perspective. *J Biomech.* 2003; 36:1409–1424. [PubMed: 14499290]
7. Kapur S, Baylink DJ, Lau KHW. Fluid flow shear stress stimulates human osteoblast proliferation and differentiation through multiple interacting and competing signal transduction pathways. *Bone.* 2002; 32:241–251.
8. McAllister T. Fluid shear stress stimulates prostaglandin and nitric oxide release in bone marrow-derived preosteoclast-like cells. *Biochem Bioph Res Co.* 2000; 270:643–648.
9. Li J, Rose E, Frances D, Sun Y, You L. Effect of oscillating fluid flow stimulation on osteocyte mRNA expression. *J Biomech.* 2012; 45:247–251. [PubMed: 22119108]
10. Nauman EA, Satcher RL, Keaveny TM, Halloran BP, Bikle DD. Osteoblasts respond to pulsatile fluid flow with short-term increases in PGE2 but no change in mineralization. *J Appl Physiol.* 2001; 90:1849–1854. [PubMed: 11299276]
11. Klein-Nulend J, Semeins CM, Burger EH. Prostaglandin mediated modulation of transforming growth factor-beta metabolism in primary mouse osteoblastic cells in vitro. *J Cell Physiol.* 1996; 168:1–7. [PubMed: 8647903]
12. Coughlin TR, Niebur GL. Fluid shear stress in trabecular bone marrow due to low-magnitude high-frequency vibration. *J Biomech.* 2012; 45:2222–2229. [PubMed: 22784651]
13. Rubin J, Rubin C, Jacobs CR. Molecular pathways mediating mechanical signaling in bone. *Gene.* 2006; 367:1–16. [PubMed: 16361069]
14. Ziambaras K, Lecanda F, Steinberg TH, Civitelli R. Cyclic stretch enhances gap junctional communication between osteoblastic cells. *J Bone Miner Res.* 1998; 13:218–228. [PubMed: 9495514]
15. Litzenberger JB, Kim JB, Tummala P, Jacobs CR. Beta1 integrins mediate mechanosensitive signaling pathways in osteocytes. *Calcif Tissue Int.* 2010; 86:325–332. [PubMed: 20213106]
16. Malone AM, Anderson CT, Tummala P, Kwon RY, Johnston TR, Stearns T, Jacobs CR. Primary cilia mediate mechanosensing in bone cells by a calcium-independent mechanism. *Proc Natl Acad Sci U S A.* 2007; 104:13325–13330. [PubMed: 17673554]
17. Hoey DA, Tormey S, Ramcharan S, O’Brien FJ, Jacobs CR. Primary cilia-mediated mechanotransduction in human mesenchymal stem cells. *Stem Cells.* 2012; 30:2561–2570. [PubMed: 22969057]
18. Wheatley DN, Wang AM, Strugnell GE. Expression of primary cilia in mammalian cells. *Cell Biol Int.* 1996; 20:73–81. [PubMed: 8936410]
19. Sorokin S. Centrioles and the formation of rudimentary cilia by fibroblasts and smooth muscle cells. *J Cell Biol.* 1962; 15:363–377. [PubMed: 13978319]

20. Kobayashi T, Dynlacht BD. Regulating the transition from centriole to basal body. *J Cell Biol.* 2011; 193:435–444. [PubMed: 21536747]
21. Gerdes JM, Davis EE, Katsanis N. The vertebrate primary cilium in development, homeostasis, and disease. *Cell.* 2009; 137:32–45. [PubMed: 19345185]
22. Schwartz EA, Leonard ML, Bizios R, Bowser SS. Analysis and modeling of the primary cilium bending response to fluid shear. *Am J Physiol.* 1997; 272:F132–F138. [PubMed: 9039059]
23. Praetorius HA, Spring KR. Bending the MDCK cell primary cilium increases intracellular calcium. *J Membr Biol.* 2001; 184:71–79. [PubMed: 11687880]
24. Hoey DA, Kelly DJ, Jacobs CR. A role for the primary cilium in paracrine signaling between mechanically stimulated osteocytes and mesenchymal stem cells. *Biochem Biophys Res Commun.* 2011; 412:182–187. [PubMed: 21810408]
25. Temiyasathit S, Tang WJ, Leucht P, Anderson CT, Monica SD, Castillo AB, Helms JA, Stearns T, Jacobs CR. Mechanosensing by the primary cilium: deletion of Kif3A reduces bone formation due to loading. *PLoS ONE.* 2012; 7:e33368. [PubMed: 22428034]
26. Qiu N, Xiao Z, Cao L, Buechel MM, David V, Roan E, Quarles LD. Disruption of Kif3a in osteoblasts results in defective bone formation and osteopenia. *J Cell Sci.* 2012; 125:1945–1957. [PubMed: 22357948]
27. Bodle JC, Rubenstein CD, Phillips ME, Bernacki SH, Qi J, Banes AJ, Lobo EG. Primary cilia: the chemical antenna regulating human adipose-derived stem cell osteogenesis. *PLoS ONE.* 2013; 8:e62554. [PubMed: 23690943]
28. Whitfield JF. The solitary (primary) cilium—a mechanosensory toggle switch in bone and cartilage cells. *Cell Signal.* 2008; 20:1019–1024. [PubMed: 18248958]
29. Gardner K, Arnoczky SP, Lavagnino M. Effect of in vitro stress-deprivation and cyclic loading on the length of tendon cell cilia in situ. *J Orthop Res.* 2011; 29:582–587. [PubMed: 20957738]
30. McGlashan SR, Knight MM, Chowdhury TT, Joshi P, Jensen CG, Kennedy S, Poole CA. Mechanical loading modulates chondrocyte primary cilia incidence and length. *Cell Biol Int.* 2010; 34:441–446. [PubMed: 20100169]
31. Tonna EA, Lampen NM. Electron microscopy of aging skeletal cells. I. Centrioles and solitary cilia. *J Gerontol.* 1972; 27:316–324. [PubMed: 5046597]
32. Uzbekov RE, Maurel DB, Aveline PC, Pallu S, Benhamou CL, Rochefort GY. Centrosome fine ultrastructure of the osteocyte mechanosensitive primary cilium. *Microsc Microanal.* 2012; 18:1430–1441. [PubMed: 23171702]
33. Praetorius HA, Spring KR. The renal cell primary cilium functions as a flow sensor. *Curr Opin Nephrol Hypertens.* 2003; 12:517–520. [PubMed: 12920399]
34. Tenenbaum, HC. Cellular origins and theories of differentiation of bone-forming cells. In: Hall, BK., editor. *Bone: The osteoblast and osteocyte.* CRC Press; Boca Raton: 1992. p. 41–69.
35. Chang MK, Raggatt LJ, Alexander KA, Kuliwaba JS, Fazzalari NL, Schroder K, Maylin ER, Ripoll VM, Hume DA, Pettit AR. Osteal tissue macrophages are intercalated throughout human and mouse bone lining tissues and regulate osteoblast function in vitro and in vivo. *J Immunol.* 2008; 181:1232–1244. [PubMed: 18606677]
36. Weiss L, Geduldig U. Barrier cells: stromal regulation of hematopoiesis and blood cell release in normal and stressed murine bone marrow. *Blood.* 1991; 78:975–990. [PubMed: 1868254]
37. Turner CH, Owan I, Alvey T, Hulman J, Hock JM. Recruitment and proliferative responses of osteoblasts after mechanical loading in vivo determined using sustained-release bromodeoxyuridine. *Bone.* 1998; 22:463–469. [PubMed: 9600779]
38. Tummala P, Arnsdorf EJ, Jacobs CR. The role of primary cilia in mesenchymal stem cell differentiation: a pivotal switch in guiding lineage commitment. *Cell Mol Bioeng.* 2010; 3:207–212. [PubMed: 20823950]
39. Fritton JC, Myers ER, Wright TM, van der Meulen MC. Loading induces site-specific increases in mineral content assessed by microcomputed tomography of the mouse tibia. *Bone.* 2005; 36:1030–1038. [PubMed: 15878316]
40. Bayraktar HH, Morgan EF, Niebur GL, Morris GE, Wong EK, Keaveny TM. Comparison of the elastic and yield properties of human femoral trabecular and cortical bone tissue. *J Biomech.* 2004; 37:27–35. [PubMed: 14672565]

41. Poole, T., Stayner, C., McGlashan, SR., Parker, K., Wiles, A., Jennings, M., Jensen, CG., Johnstone, AC., Walker, RJ., Eccles, MR. Primary cilia defects in the polycystic kidneys from an ovine model of Meckel Gruber syndrome. First International Cilia in Development and Disease Scientific Conference; London. 2012.
42. Poole CA, Zhang ZJ, Ross JM. The differential distribution of acetylated and detyrosinated alpha-tubulin in the microtubular cytoskeleton and primary cilia of hyaline cartilage chondrocytes. *J Anat.* 2001; 199:393–405. [PubMed: 11693300]
43. Xiao Z, Zhang S, Mahlios J, Zhou G, Magenheimer BS, Guo D, Dallas SL, Maser R, Calvet JP, Bonewald L, Quarles LD. Cilia-like structures and polycystin-1 in osteoblasts/osteocytes and associated abnormalities in skeletogenesis and Runx2 expression. *J Biol Chem.* 2006; 281:30884–30895. [PubMed: 16905538]
44. McNamara LM, Majeska RJ, Weinbaum S, Friedrich V, Schaffler MB. Attachment of osteocyte cell processes to the bone matrix. *Anat Rec (Hoboken).* 2009; 292:355–363. [PubMed: 19248169]
45. Besschetnova TY, Kolpakova-Hart E, Guan Y, Zhou J, Olsen BR, Shah JV. Identification of signaling pathways regulating primary cilium length and flow-mediated adaptation. *Curr Biol.* 2010; 20:182–187. [PubMed: 20096584]

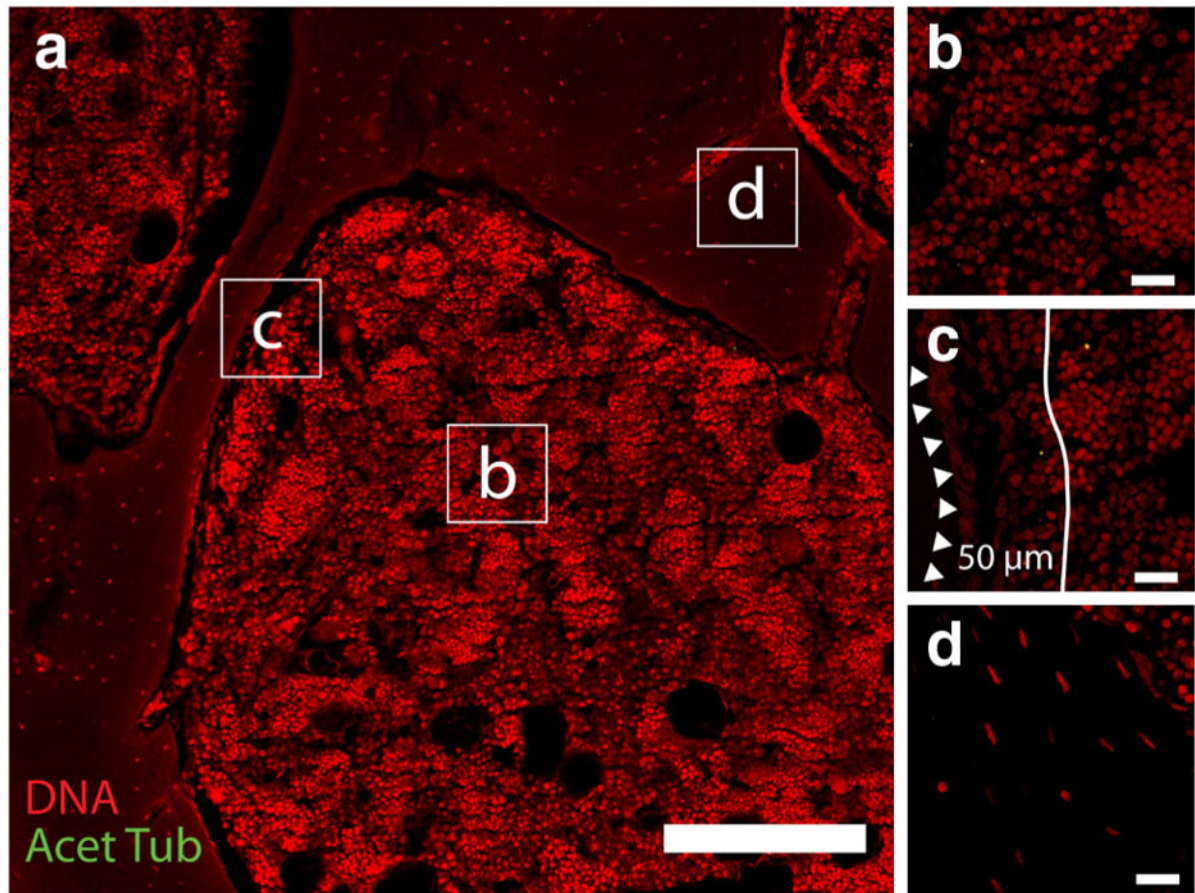


**Fig. 1.**

**a** Ovine trabecular bone pores averaged approximately 0.5 mm across (*scale* = 200 μm). Primary cilia stained by an acetylated  $\alpha$ -tubulin antibody (*green*) were measured and quantified in four distinct locations of the trabecular bone compartment: **b** marrow space more than 50 μm from the bone surface, **c** marrow within 50 μm of the bone surface, in the bone lining cells, and **d** in osteocytes (*scale* = 20 μm) (Color figure online)

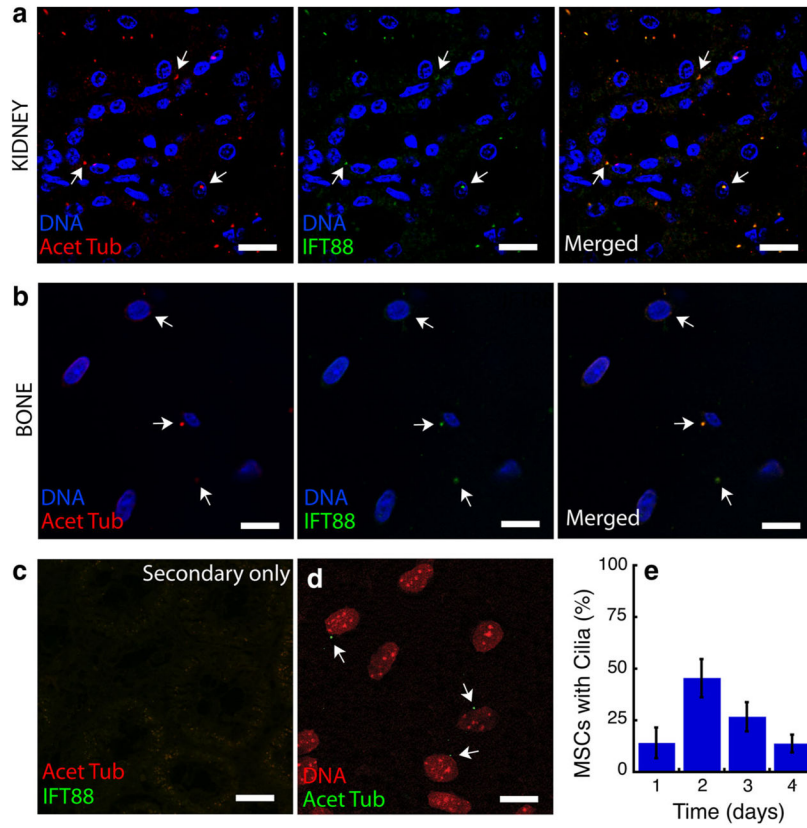


**Fig. 2.** Primary and secondary antibodies were validated for sensitivity and specificity in ovine cells and tissues. **a** The ovine kidney collecting duct, which is known to express primary cilia ubiquitously, was stained by both anti acetylated  $\alpha$ -tubulin and by anti IFT88, two markers expressed in the primary cilium (*scale* = 20  $\mu$ m). The image is a single confocal slice of the immunostained section. Nearly all cells exhibited cilia stained by both antibodies. The colocalization of staining validates the sensitivity of the antibody for cilia. **b** Primary cilia in trabecular bone were similarly stained by both anti acetylated  $\alpha$ -tubulin and by anti IFT88 (*scale* = 20  $\mu$ m). **c** Ovine kidney was immunostained with only secondary antibodies to ensure specificity for the primary antibodies (*scale* = 20  $\mu$ m). **d** In cell culture, ovine bone marrow stromal cells cultured to passage three displayed primary cilia that were positive for acetylated  $\alpha$ -tubulin (*scale* = 20  $\mu$ m, *N* = 3). **e** The number of primary cilia in the expanding cells varied across 4 days of culture (*N* = 3)

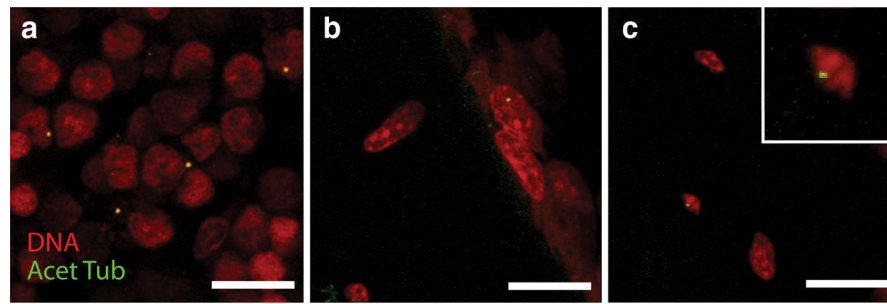


**Fig. 3.** Positive acetylated  $\alpha$ -tubulin stained cilia were counted in **a** the marrow, **b** bone lining cells, and **c** osteocytes (*scale* = 10  $\mu$ m)

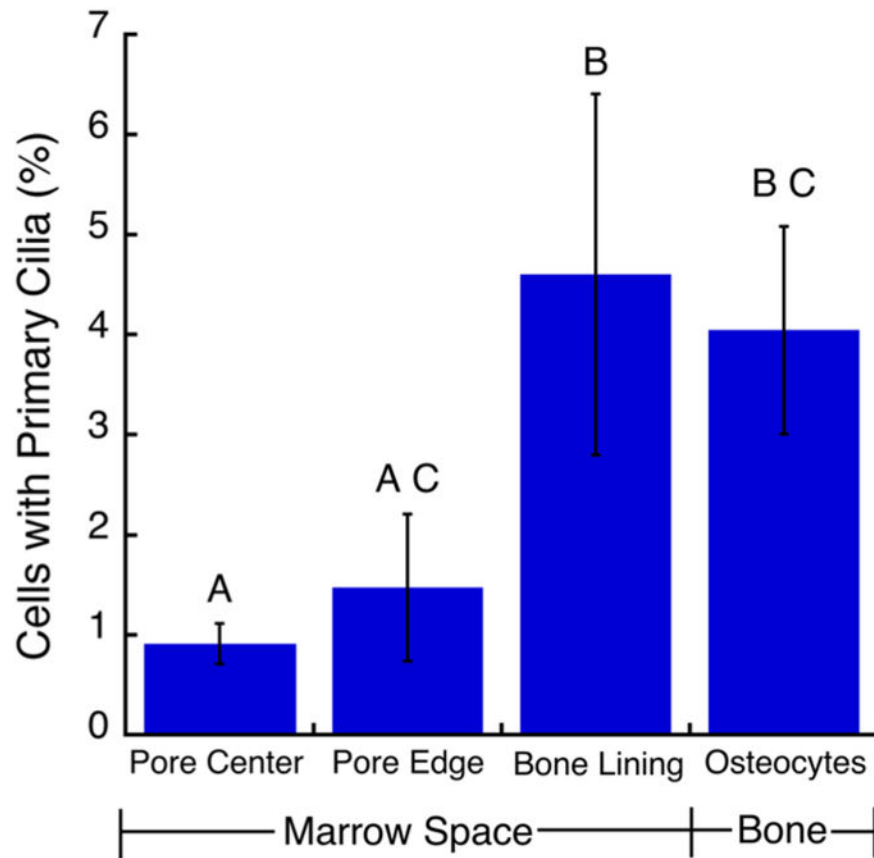


**Fig. 4.** Osteocytes and bone lining cells had a higher incidence of cilia expression (defined as cilia greater than 1  $\mu\text{m}$  in length) than cells in the central marrow cavity more than 50  $\mu\text{m}$  from the bone surface. Bars marked by the *same letter* are not statistically different ( $N=3$ ; mean  $\pm$  STDEV;  $p < 0.05$ , ANOVA with Tukey's HSD)

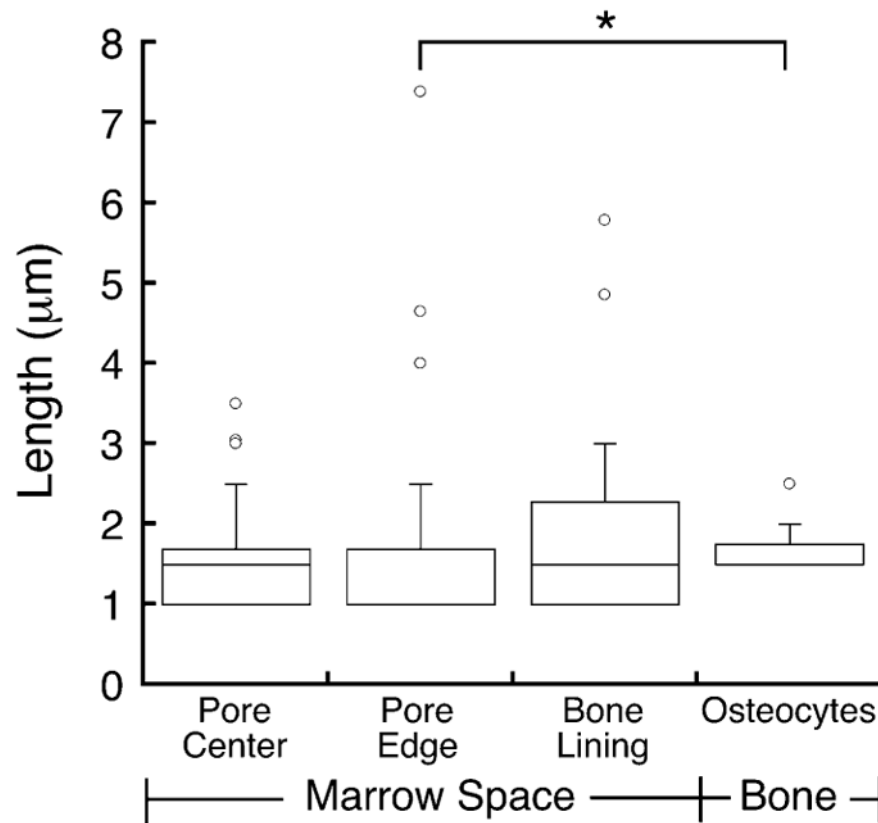


**Fig. 5.** The average length of primary cilia was 1.49  $\mu\text{m}$  in marrow cells away from the endosteal surface, 1.46  $\mu\text{m}$  in marrow cells near the bone surface, 1.86  $\mu\text{m}$  for the bone lining cells, and 1.65  $\mu\text{m}$  for the osteocytes. Cilia were longer in osteocytes than in cells in the marrow near the bone surface ( $*p < 0.05$ , Kruskal–Wallis). The *box* represents the upper and lower quartiles, the middle bar is the median, and whiskers span the 95th percentile. *Circles* represent outliers